Figures:

Figure 1:

Hyaline membrane formation in lung of an adult male unexpectedly dying during the seasonal surge of influenza in February 1977 following major surgery on his larynx (removal of polyps of the vocal chords). The active inflammation is partially a result of the continuing presence of the virus in the lesions. Here the membrane has partially collapsed into the exudate.

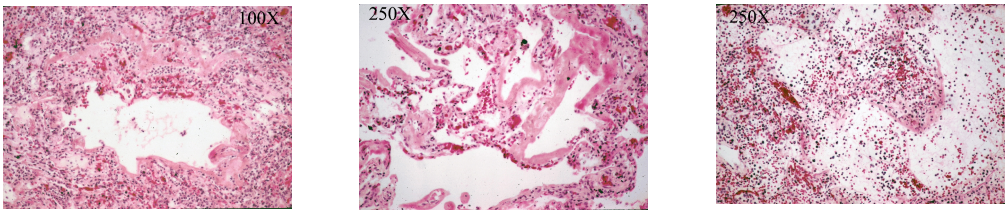

Figures 2:

Fresh (unfixed) and post fixation autopsy specimens from premature infants. Photograph, left: fresh autopsy lungs from a premature newborn with clinical respiratory distress syndrome; photograph, right: a fixed lung showing indentations from the rib cage.

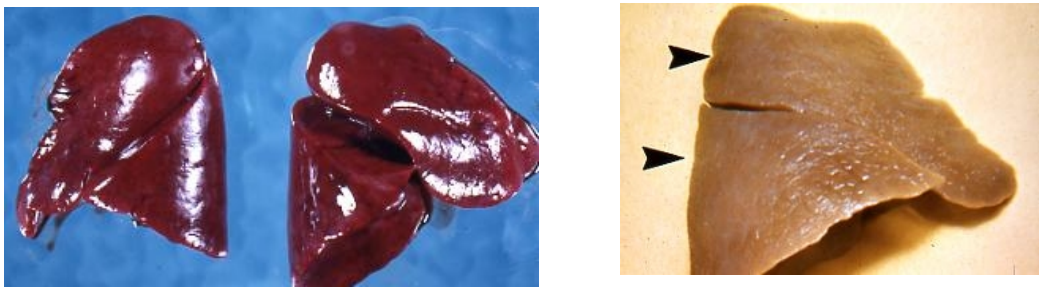

Figure 3:

Photomicrographs, left to right: a midplane section of a lobule with *air bronchogram* and compressed protein and cell nuclei at two foci, [1] at the bifurcation of a bronchus and [2] in the distal alveolar duct. Premature lungs at this age do not have terminal alveoli. Full alveolization is not complete until around 16 years of age. The format of these two lesion subtypes are those of a chemical burn, coagulation necrosis and compression of exudate. Very similar findings are seen in the lungs after phosgene poisoning (war gas) and inhalation of very hot gases, like that of the notorious Cocoanut Grove disaster of 1942 in Boston [*Am.J.Pathol*. 21:311-332, 1945].

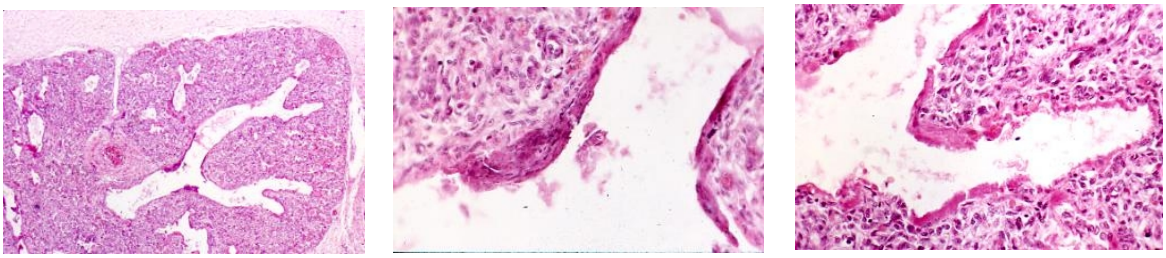

Figure 4:

From a University of Florida Student Research paper (see references). Grading of the four lesion components was from 0 to 4+, congestion, atelectasis, airspace edema, and membrane formation. The graph is based on time sequence cumulative grade per component which shows: [1] the known dominance of congestion (or hyperemia) in the pulmonary response, [2] a distinctive acceleration of the cumulative grade begins at 5-6 hours and sharply shifts to plateau format at ten hours, except for membrane formation, and [3] further enhancement of all four over the final two hours, 17 and 18, the maximum survival in this control subset (N = 15).

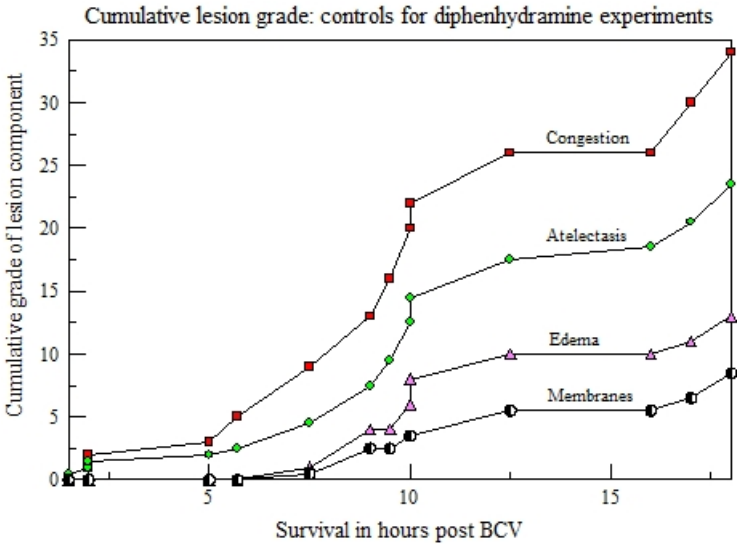

Figure 5:

From: On the pulmonary toxicity of oxygen. I. The relationship of oxygen content to the effects of oxygen on the lung. *Lab. Invest.* 21: 439-448, 1969. The usual convention of arrangement for the abscissa and ordinate have been reversed in order to display the third dimension of total pressure in a more effective pattern, rising from the assigned X-axis in sub-Figure 2 and also in sub-Figure 3 by which to match that array. It is apparent that the reciprocal per cent concentration of oxygen and nitrogen is quantitatively related to the extent of lung injury in animal groups of 25, 30, or more newborn rabbits with ventilatory distress following bilateral cervical vagotomy.

The evidence that oxygen is the etiologic force for hyaline membrane disease

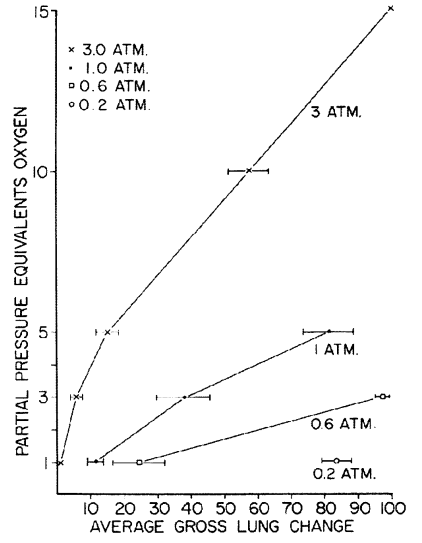

FIG. 2. Relationship of oxygen by partial pressure equivalent (*PPE*) to lung lesions. The limits of mean ± standard error of the mean have been omitted for clarity on this point: 3.0 atm. abs., 1 *PPE* (0.5 ± 0.7 per cent). The point 3.0 atm. abs., 15 *PPE* is unique (100 ± 0.0 per cent).

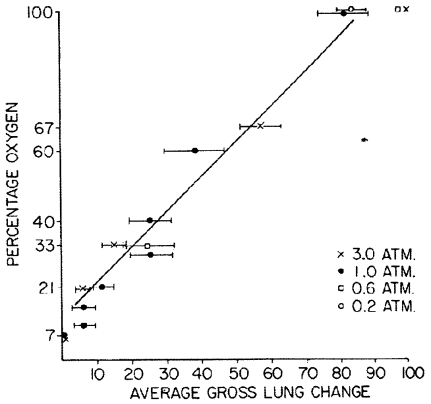

FIG. 3. Relationship of oxygen by percentage to lung lesions. The limits of mean ± standard error of the mean have been omitted for clarity on these points: (1) 0.6 atm. abs., 100 per cent oxygen (97.2 ± 2.2 per cent); (2) 1.0 atm. abs., 7 per cent oxygen (0.2 ± 0.2 per cent); and (3) 3.0 atm. abs., 7 per cent oxygen (0.5 ± 0.7 per cent). The point 3.0 atm. abs., 100 per cent oxygen is unique (100 ± 0.0 per cent).

Figure 6.

Three gross views of newborn rabbit lungs from different treatments after vagotomy. Far left: segmental apical hepatization, 7% oxygen in argon. Middle: bilateral recurrent laryngeal neurectomy in 100% oxygen. Far right: thoracic restraint in air.

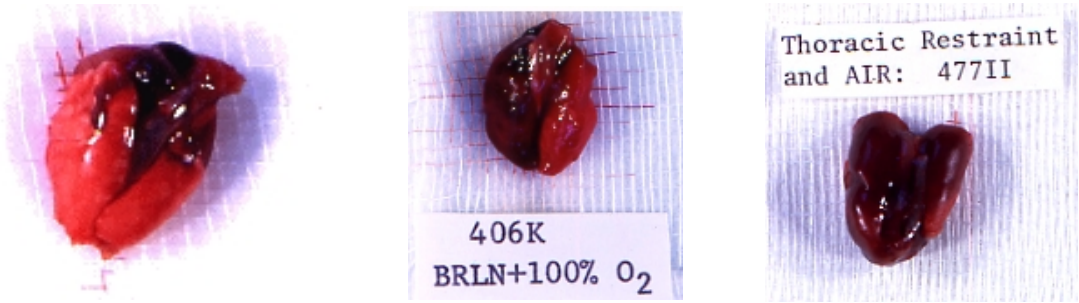

Figure 7.

Semilog plot of the extent of lung injury from oxygen levels from 3% to 21% with nitrogen, helium, and sulfur hexafluoride as diluent. The minimum occurred with 7% oxygen in nitrogen, 0.2% (heavy black line, lowest curve). Comparable minimums are seen in 7% oxygen when the diluent is sulfur hexafluroide (middle red line), and helium (upper thin black line). The semilog plot minimizes the nadir of the helium curve and exaggerates that for nitrogen. Values for the top oxygen percentage are 21% for nitrogen (air) and 20% for both sulfur hexafluoride and helium.

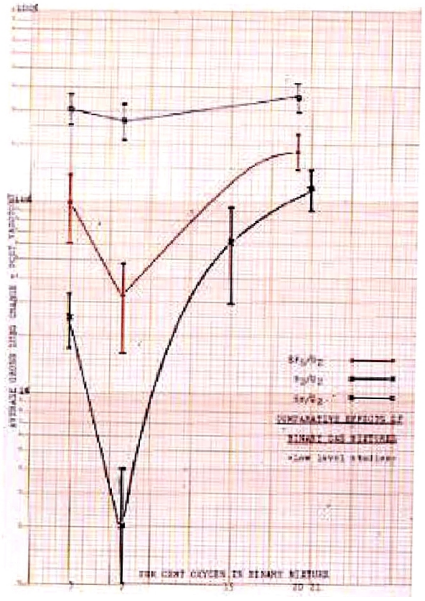

Figure 8.

Combination plot of extent of lung injury (ordinate), after BCV and without BCV against the saturation of the outer electron shell(s) of the atoms (helium and argon), the diatomic molecules (hydrogen and nitrogen), and the compound molecule (sulfur hexafluoride).

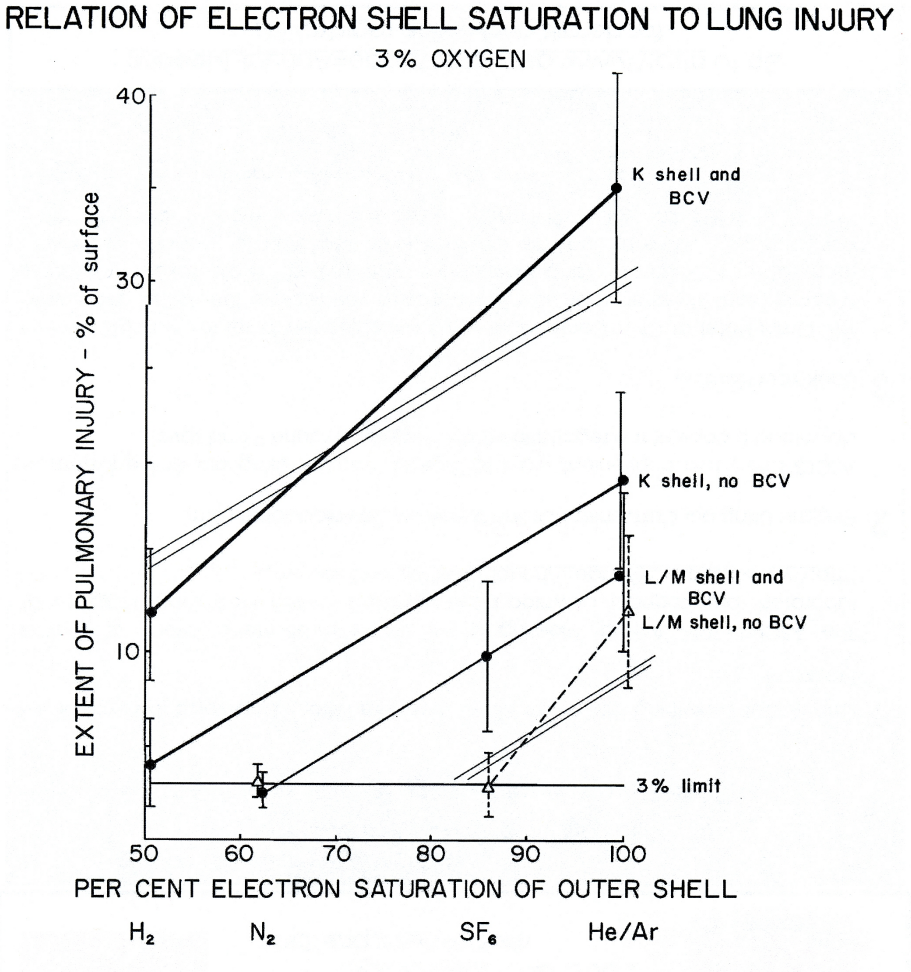

Figure 9.

Graphical comparison between post-BCV lung injury by diluent gas (left) and parallel non-BCV (right) runs with the same diluents at 3% oxygen. This shows the additive effect of respiratory distress induced by BCV, expanding the left vertical plot while maintaining the relative position of the effects.

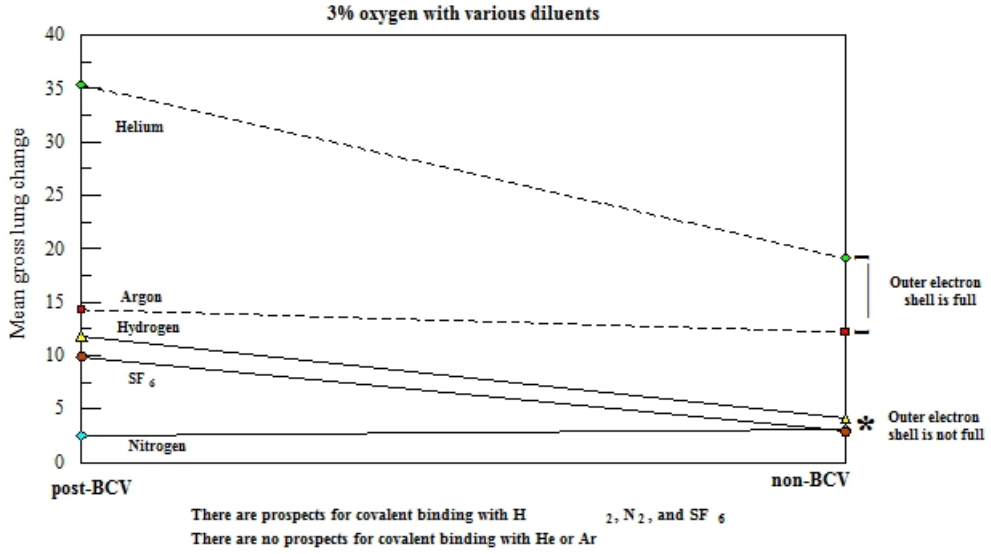

Figure 10.

Survival plots of newborn rabbits subjected to thoracic restraint. Air only, green circles; 100% oxygen, red squares. The curves essentially superimpose for the interval 40-70 hours with a slight difference during the third phase while terminating at very similar time points, more or less around 100 hours.

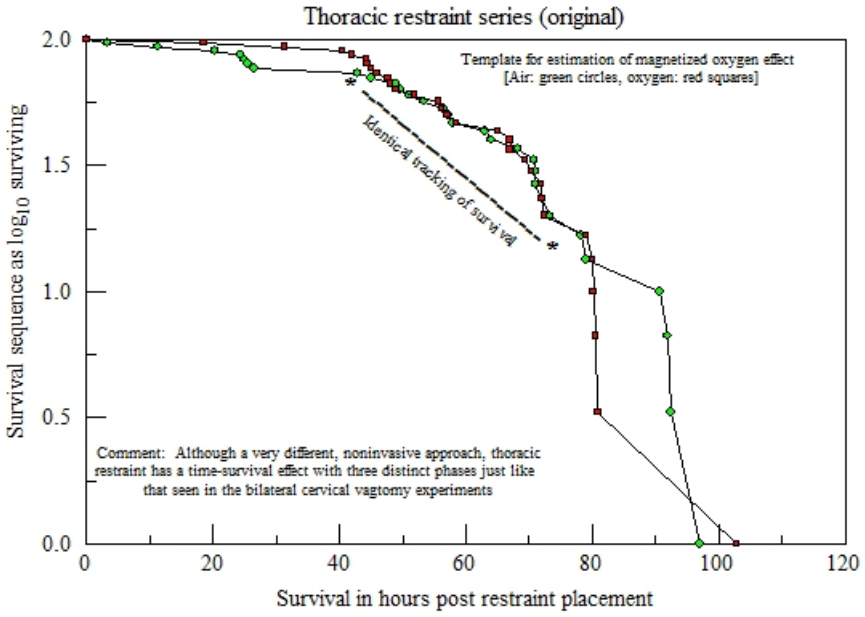

Figure 11.

Survival plot of newborn rabbits with induced respiratory distress by thoracic restraint subjected to the flow of 100% oxygen at 1.0 L/min in sealed chambers. Plain 100% oxygen, green circles; magnetized 100% oxygen, red squares. The terminal end points are the same, suggestive of a maximal tolerable effect on body weight loss through metabolic acidosis and glycogen depletion. Plain 100% oxygen, green circles; magnetized 100% oxygen, red squares.

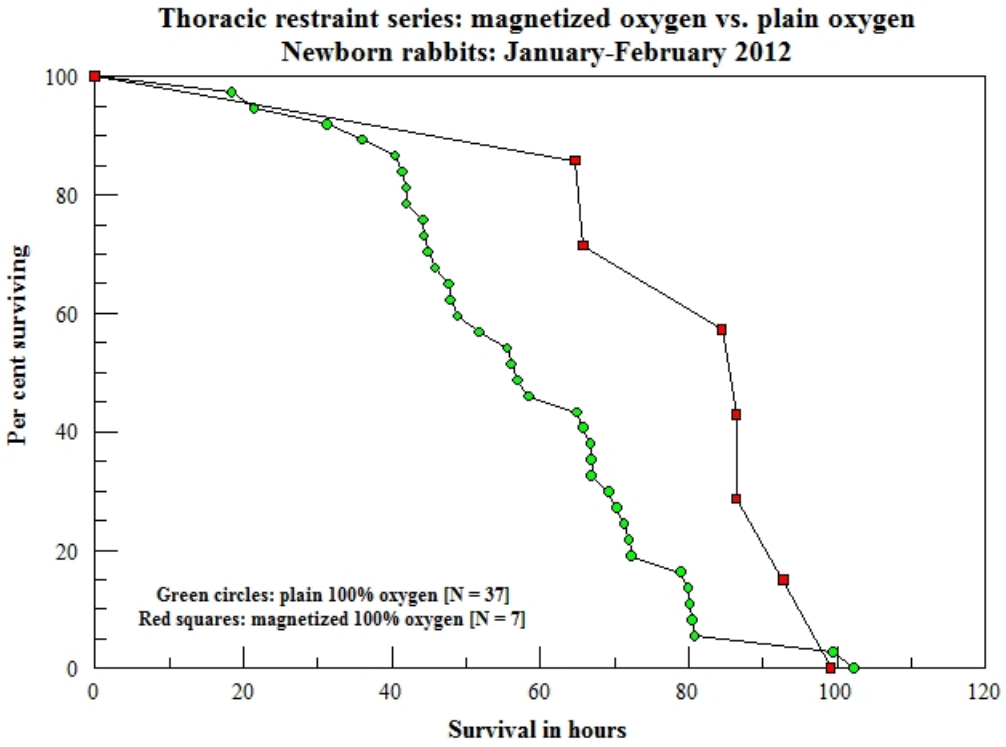

Figure 12.

Photograph of 480 ml sealed mouse chamber, maximum capacity four animals, resting on a grid of four donut ceramic magnets during oxygen feed. Gas flow exits on the far side through holes too small for the nose of the mice and approximating the cross section of the intake tubing. After removal of dead animals the chamber was flushed with oxygen at 5 L/min for several minutes.

Figure 13:

Survival plot of female adult white mice subjected to the flow of 100% oxygen at 1.0 L/min in sealed chambers. Plain 100% oxygen, green circles; magnetized 100% oxygen, red squares. The terminal end points are the same, suggestive of a maximal tolerable effect on body weight loss through metabolic acidosis and glycogen depletion.